Heliyon 7 (2021) e05962

Contents lists available at ScienceDirect

Heliyon

journal homepage: www.cell.com/heliyon

Research article

Synthesis, structural characterization, computational studies and stability evaluations of metal ions and ZnONPs complexes with dimercaptosuccinic acid

Poonyawee Keattanong [a], Nootcharin Wasukan [b], Mayuso Kuno [a], Sujittra Srisung [a,*]

[a] Department of Chemistry, Faculty of Science, Srinakharinwirot University, Sukhumwit 23, Wattana District, Bangkok, 10110, Thailand
[b] National Science and Technology Development Agency (NSTDA), 111 Thailand Science Park, Khlong Luang, Pathum Thani, 12120, Thailand

ARTICLE INFO

Keywords:
Meso-2,3-dimercaptosuccinic acid (DMSA)
Metal complex
Zinc oxide nanoparticles (ZnONPs)
Stability constant
Computational chemistry

ABSTRACT

Meso-2,3-dimercaptosuccinic acid (DMSA) is one of the efficient chelating reagents for treating the toxicity of several heavy metals. Currently, nanomaterial have been applied to various parts including zinc Oxide nanoparticles (ZnONPs). ZnONPs have several properties and are used as many applications. An increasing the amount of ZnONPs in commercial products causes risks related to free radicals or reactive oxygen species (ROS) in the body, leading to oxidative stress and eventually to the cancer process. In the present work, we mainly focused on the study of DMSA complexes in term of metal ions and nanoparticles. The synthesis of DMSA-ZnONPs by the co-precipitation method were determined, followed by Scanning Electron Microscope, Fourier Transform Infrared Spectroscopy and UV-Vis spectrophotometry confirming successful synthesis process. The stability study of the DMSA complexes with metal ions and ZnONPs were determined and evaluated the stability constant (K), with the Benesi- Hildebrand equation. All complexes with DMSA were formed at a 1:2 ratio by the dithiol group and the carboxyl group with different stability constants. Therefore, these results can help of an understanding of the interaction and its behavior between DMSA with heavy metal ion and ZnONPs. In addition, the stable structure of DMSA and metal ion complexes were predicted using the B3LYP and the 6-31G (d,p) basis set which the most stable structure of *meso*-DMSA was 2R,3S conformation and the metal ions and DMSA complexes was complex 2a with the binding energy of -1553.46 kcal mol^{-1}.

1. Introduction

Nowadays, technological advances make the manufacturing of goods and materials faster (Vance et al., 2015; Ramos et al., 2017). As a result, both ecosystems and human beings are at risk of exposure to pollutants from the manufacturing industry, and in different components and into the body, respectively (Jeevanandam et al., 2018; Khan et al., 2019). Heavy metals are widely used in the manufacturing industry and contaminate the environment, including the soil, water, and air vapors, through leakages or direct release (Bradl, 2002; He et al., 2005; Ali et al., 2019; Sfakianakis et al., 2015; Arunakumara et al., 2013). In daily life, human beings can be exposed to such chemicals through a wide range of activities, either directly and indirectly and in small quantities. However, accumulation in tissues and organs over a long period of time may have seriously adverse health effects (Lorenz et al., 2012).

In addition, zinc oxide nanoparticles (ZnONPs) are known to be one of the most multifunctional nanoparticles due to its a wide range of properties, such as piezoelectric, ferromagnetic, photoluminescent, electroluminescent, and as chemical sensors and biosensors (Willander, 2014; Fortunato et al., 2009; Alamdari et al., 2020). It is also widely used in the textile industry and for electronic devices. There is a tendency towards higher levels of production and product development. For this reason, both consumers and the workers manipulating these products are at risk of allowing heavy metals and nanoparticles into the body. Many studies have been conducted on the effects of heavy metals on humans that both heavy metals and ZnONPs caused an increasing in the amounts of free radicals or reactive oxygen species (ROS) in the body, leading to oxidative stress. At the same time, free radicals play an important role in the cancer process, resulting in cancer cells becoming more abundant (Lee et al., 2007).

* Corresponding author.
E-mail address: sujittras@g.swu.ac.th (S. Srisung).

https://doi.org/10.1016/j.heliyon.2021.e05962
Received 4 September 2020; Received in revised form 12 November 2020; Accepted 8 January 2021

Succimer or dimercaptosuccinic acid (DMSA) has two diastereomers, *meso* form (2R,3S isomer) and the racemic mixture (2S,3S and 2R,3R isomers) (Rivera et al., 1989; Fang et al., 1996). Whereas, *meso*-DMSA form (Figure 1) is available commercially and used clinically, which gets attention for treating heavy metals and nanoparticles intoxication in human beings (Cavanillas et al., 2012; Jahromi et al., 2014). *meso*-DMSA has been used in most published investigations of potential therapeutic drug for heavy metals removal due to its used as a chelating agent (Aposhian et al., 1995; Campbell et al., 1986). Therefore, the *meso*-DMSA form was carried out in this work. We mainly focused on the studies of DMSA complexes in term of metal ions and nanoparticles. The synthesis of DMSA-ZnONPs by cost effective and simple co-precipitation methods were determined. Then, characterized by Scanning Electron Microscopy (SEM), Fourier Transform Infrared Spectroscopy (FTIR) and UV-Vis spectroscopy. In addition, the stability determination of DMSA complex with ZnONPs and other heavy metal by UV-Vis titration were determined.

In addition, the computational methods using the density functional theory (DFT) was applied for a calculated model in terms of the DMSA-metal complexes. Because no information was shown on the interaction of Zn(II)-DMSA, Ni(II)-DMSA and Fe(II)-DMSA complexes that were of interest to this study. Therefore, the theoretical calculations based on quantum mechanics were investigated to compose reliable predictions. This calculation could be used to explain the stable foundation of molecular structures, energy and other parameter properties.

Consequently, the main objectives were to determine the interaction parameters, the binding energy of complexes, as well as the details on the experimental results. The geometry optimization, the frequency of these structures and binding energies were determined using density functional approaches B3LYP method and the 6-31G (d,p) basis set.

2. Experimental section

2.1. Materials

Meso-2,3-dimercaptosuccinic acid (DMSA) (98%) was purchased from Sigma Aldrich (St. Louis, MO). 4-(2-hydroxyethyl)-1-piperazineethanesulfonic acid (HEPES) was obtained from Fisher Scientific (Washington, D.C.) for adjusting the pH. The $ZnCl_2$, $NiCl_2.6H_2O$ and $FeSO_4.7H_2O$ were purchased from Carlo Erba Reagents (Italy). The heavy metal solutions, containing Zn, Ni and Fe for adsorption tests, were prepared by diluting the stock solution to the desired concentrations with distilled water. The ZnONPs and DMSA-ZnONPs complexes were synthesized according to the methods in our previous work (Rao and Rao, 2015).

2.2. Physical measurements

For the experimental details, the absorption spectra of ZnONPs, DMSA-ZnONPs complex and the other metal complex were recorded by a Shimadzu UV-2401PC UV–Vis spectrophotometer working in the range of 200–800 nm. The spectrum was recorded using 1.0 cm quartz cuvettes that has a slit width of 1.0 nm at room temperature. The IR spectrum of samples were recorded on a Perkin Elmer FT-IR spectrum BX spectrometer in the region of 4000–400 cm^{-1} in solid state. Each sample was conducted under identical conditions with triplicated of experiments. The characterization of morphology for ZnONPs and DMSA-ZnONPs complex were coated with Platinum using the Q150R S QUORUM coater prior to investigation by using Field Emission Scanning Electron Microscope (JSM-7610F).

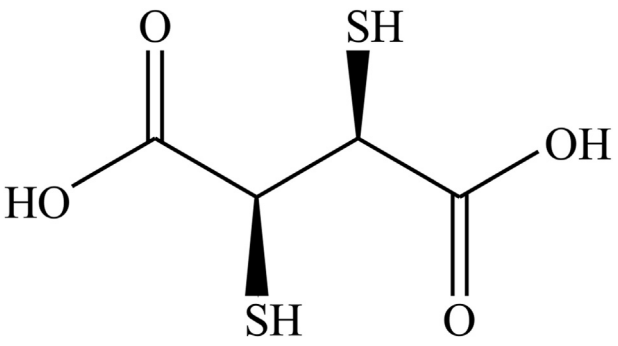

Figure 1. Structure of *meso*-DMSA.

2.3. Syntheses

2.3.1. Synthesis and characterize ZnONPs

In this experiment, 25 ml of 0.4 M zinc chloride ($ZnCl_2$) in ethanol solution and 10 ml of 0.8 M potassium hydroxide (KOH) in ethanol solution were stirred for one hour. The 0.8 M KOH for 10 ml was slowly added (drop by drop for 45 min), and the procedure was performed through constant stirring at room temperature. After complete addition, the round bottom flask was sealed and stirred overnight at room temperature. The material formed solution was centrifuged for 10 min to separate the precipitate. Then, the solution was filtered and washed in five times with ethanol and five times with deionized water. Finally, the solution was dried in a vacuum oven at 100 °C for four hours, and the $Zn(OH)_2$ was completely converted into ZnONPs (Rao and Rao, 2015). The synthesized ZnONPs was characterized by scanning electron microscope (SEM), Fourier Transform Infrared Spectrometer (FTIR) and UV-Vis spectrometer.

2.3.2. Synthesis and characterize DMSA-ZnONPs complex

In this experiment, each solution in ethanol of the 25 ml of 0.4 M zinc chloride ($ZnCl_2$), 1 ml of 0.8 M *meso*-2,3-dimercaptosuccinic acid (DMSA) and 10 ml of 0.8 M Potassium Hydroxide (KOH) were stirred for one hour. The mixture of 25 ml of 0.4 M $ZnCl_2$ solution and 1 ml of 0.8 M DMSA solution was stirred for one hour. Then, 10 ml of 0.8 KOH was slowly added (drop by drop for 45 min), and the procedure was performed under constant stirring at room temperature. After the addition was complete, the round bottom flask was sealed and stirred overnight at room temperature. The formed material in the solution was centrifuged for 10 min to separate the precipitate. Then, the solution was filtered and washed with ethanol and deionized water. Finally, the solution was dried in a vacuum oven at 100 °C for four hours. The DMSA-ZnONPs was characterized by scanning electron microscope (SEM), Fourier Transform Infrared Spectrometer (FTIR) and UV-Vis spectrometer.

2.4. UV titration

2.4.1. UV titration of metal ion-DMSA complex and DMSA-ZnONPs complex

0.5 mM DMSA was prepared by dissolving 0.9 mg DMSA in 0.1 M HEPES buffer solution pH 7.4 and 1mM metal ion (Zn(II), Ni(II) or Fe(II)) solution was prepared in 10 mM HNO_3, while 1 mM ZnONPs suspension was prepared in DI water 100 ml then the suspension was sonicated before using.

All titration experiments were carried out at room temperature and monitored by the SHIMADZU UV-2401 PC spectrophotometer. For the baseline setting, 0.1 M HEPES buffer solution (pH 7.4) 2.0 ml was added into both sample and reference quartz cuvette. In each titration, solution of 2 ml of 0.5 mM DMSA in HEPES buffer solution was added to the sample cuvette, while an equal volume of HEPES buffer solution was added to reference the cuvette before recording the absorption spectra immediately. After that, aliquots of 0.2 ml, 1 mM each metal, Zn(II), Ni(II) or Fe(II) in 10 mM HNO_3 or 0.2 ml of 1 mM ZnONPs suspension after sonicated was added into the sample cuvette. An equal volume of HEPES was added into the reference cuvette before measuring the absorbance in the 200–800 nm range in the titrations of metal ions for complexation studies. The job's plot was used to calculate the formation

of metal ion-DMSA complex and the ZnONPs-DMSA complex. In addition, the determination of stability constant of metal ion-DMSA complex and ZnONPs-DMSA complex were calculated using the Benesi-Hildebrand equation.

2.5. Computational details

All calculations were performed using the Gaussian09 program package (Frisch et al., 2003). Density functional (DFT) methods were used to optimized geometries of the DMSA and its complexes with Zn(II), Ni(II) and Fe(II) metal ions. The calculations were performed using the B3LYP (B3 Becke 3-parameter exchange and Lee–Yang–Parr correlation) functional within the 6-31G (d,p) basis set for all non-metallic elements (C, O, S and H) and the 3-21G basis set for the other metal ions (Wasukan et al., 2015).

3. Results and discussion

3.1. UV–vis spectroscopic study

The ZnONPs suspension was measured by UV-Vis spectroscopic studies. The absorbance spectrum of ZnONPs showed the maximum absorbance at 362 nm (Nahhal et al., 2016) (Figure 2b). Which the $ZnCl_2$ exhibited maximum absorbance at 197.6 nm (Trivedi et al., 2017) (Figure 2a). While, the UV-Vis spectra of DMSA solutions showed the maximum absorbance at 231 nm (Figure 2c). The blue shift occurred in wavelength of maximum absorption from 362 nm to 322 nm for the complexes of DMSA-ZnONPs as shown in Figure 2d which is confirming the interaction of DMSA-ZnONPs.

3.2. FTIR spectrum

FTIR spectroscopy was performed to verify the bond structure and identify the functional group showed in Table 1 was observed in the 4000-460 cm^{-1} wavenumber range. The infrared spectroscopy measurement appears the peak at 507 cm^{-1}, corresponding to the Zn–Cl bond and remaining peaks at 1624 and 3475 cm^{-1} are due to the absorption of water molecule as shown in Figure 3a (Trivedi et al., 2017). The broad band located at 475 cm^{-1} in Figure 3b indicated that the Zn–O vibration mode that differed from the band of the Zn–Cl in Figure 3a confirming the successful synthesis of ZnONPs. In addition, the other insignificant broad bands in the spectrum were not clearly which is the absorption bands were likely related to CO_2 absorbed from the air atmosphere and can therefore be neglected (Lanje et al., 2013; Rad et al., 2019). FTIR analysis of DMSA was performed in the wavenumber range from 4000 to 460 cm^{-1} as shown in Figure 3c. The absorption peak at 2561 and 2536 cm^{-1} shows the stretching vibration of the S–H group. The absorption peaks at 1686, 1178 and 692 cm^{-1} are assigned to C=O, C–O and C–S stretching vibrations, respectively (Rivera et al., 1989; Sevinc et al., 2012; Pillai et al., 2020). Meanwhile, DMSA-ZnONPs also has the characteristic the asymmetric and symmetric stretching modes carboxylate (M(RCOO)) was attributed to a peak at 1568 and 1386 cm^{-1} in the FTIR spectrum as shown in Figure 3d. The peak at 474 cm^{-1} corresponds to the Zn–O and remaining peaks at 3377 cm^{-1} attributed to the O–H stretching are due to the absorption of water during synthesis. This result was indicated the successful production of DMSA-ZnONPs complex.

3.3. Scanning electron microscope

DMSA-ZnONPs and ZnONPs can synthesized in a variety of particle structures depending on the methods of synthesis, such as precursors, temperature, solvents and mechanochemical processes, which makes it possible to obtain products with particles that differ in shape, size and spatial structure (Kolodziejczak-Radzimska and Jesionowski, 2014). Therefore, the morphology of ZnONPs and DMSA-ZnONPs were prepared with coated Platinum with a Q150R S QUORUM coater before being measured by JSM-7610F Field Emission Scanning Electron Microscope. The ZnONPs had a well-defined flower shape with a homogeneous diameter of approximately 40 nm (Figure 4a). While the DMSA-ZnONPs had a well-defined spherical shape with a homogeneous diameter of approximately 25 nm (Figure 4b).

3.4. UV titration of metal ions-DMSA complex and ZnONPs-DMSA complex

The UV-Vis spectrum of DMSA with metal ions and ZnONPs were studied. The DMSA-Zn(II) showed a wavelength for complex 238 nm after the addition of Zn ion corresponding to the formation of metal complex as shown in Figure 5a which proposed the stoichiometric ratios in the inset of Figure 5a. The results showed that the formation of Zn(II):DMSA in ratio of 1:2 complex. For the UV-Vis spectrum for DMSA-Ni(II) showed the wavelength for complex at 311 nm in Figure 5b with

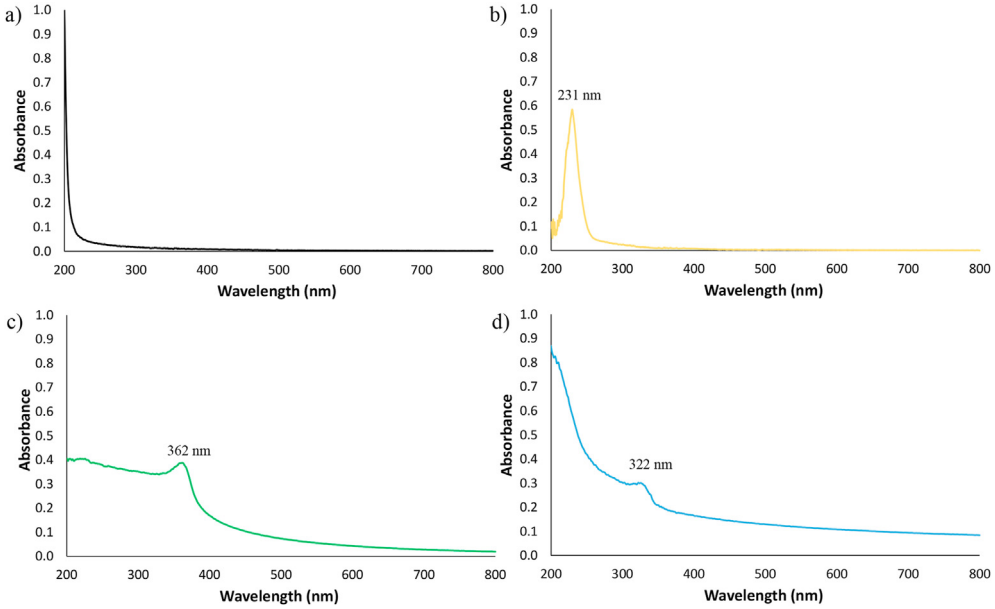

Figure 2. UV–Vis spectral of (a) $ZnCl_2$, (b) DMSA, (c) ZnONPS and (d) ZnONPs-DMSA complex in DI water solution.

Table 1. Fourier transform infrared (FTIR) vibrational wavenumbers for the $ZnCl_2$, ZnONPs, DMSA and DMSA-ZnONPs complex.

Compound	Vibrational Assignments	Wavenumber (cm^{-1})
$ZnCl_2$	Zn–Cl	507
	–OH bending	1624
	–OH stretching	3475
ZnONPs	Zn–O	475
DMSA	–SH stretching	2561, 2536
	C=O stretching	1686
	C–O stretching	1178
	C–S stretching	692
DMSA-ZnONPs complex	–OH stretching	3377
	Carboxylate (M(RCOO))	1386, 1568
	Zn–O	474

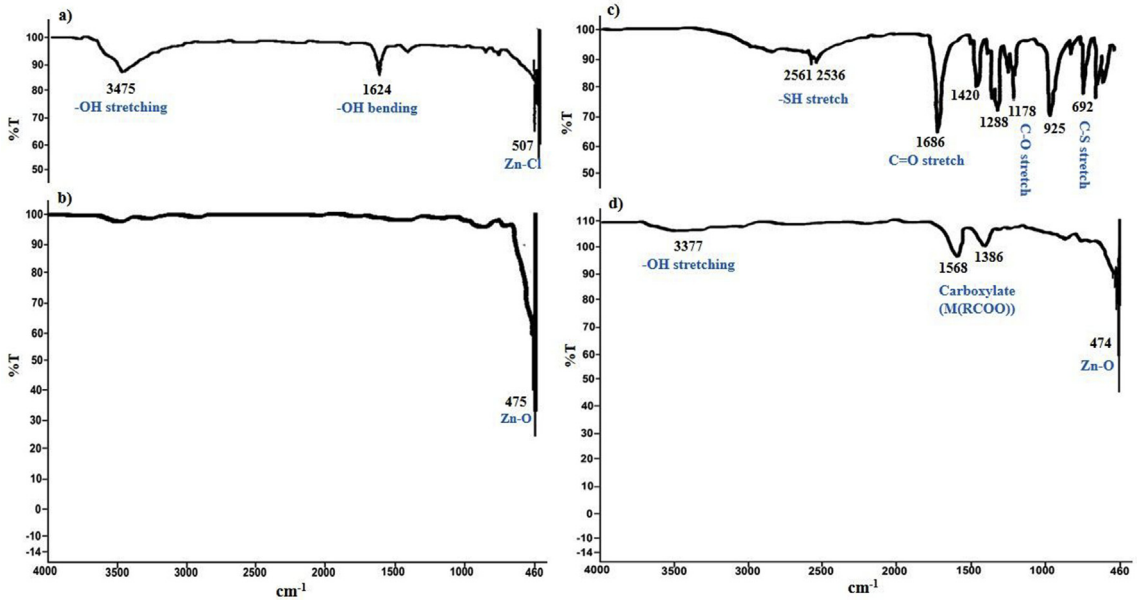

Figure 3. Fourier transform infrared (FTIR) spectra of (a) $ZnCl_2$, (b) ZnONPs, (c) DMSA and (d) DMSA-ZnONPs complex.

the formation of Ni(II) with a complex DMSA ratio of 1:2 in the inset of Figure 5b. The coordination ratio (1:2) of Ni (II) and DMSA were confirmed by UV titration. The maximum absorption spectra of DMSA exhibited absorption peak at 270 nm (Harris et al., 1991; Spuches et al., 2005). Upon the addition of the Ni(II) solutions to the DMSA ligand, the absorbance intensity of DMSA was increased, which it is a red shift and new bands appeared at 311 nm after the addition of Ni(II) solutions to the DMSA solution. The result shows a strong absorption Ni(II)-DMSA complex absorption peak at 311 nm that corresponds to electron in a occupied 3d orbitals of nickel to locate on the ligand (Biltek et al., 2003). Therefore, this result is consistent with the structure of complex as $Ni(DMSA)_2$.

In addition, the formation of DMSA-Fe(II) was confirmed at 270 nm, as shown in Figure 5c indicating the formation of Fe(II) with a complex DMSA ratio of 1:2 (Figure 5c). For the DMSA-ZnONPs, the UV-Vis spectrum showed the wavelength for complex at 235 nm that the

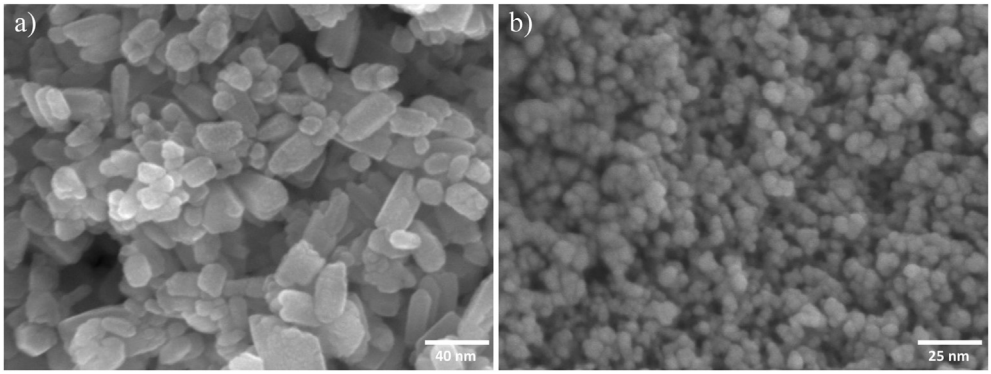

Figure 4. Scanning electron microscopy (SEM) images of (a) ZnONPs and (b) the DMSA-ZnONPs complex.

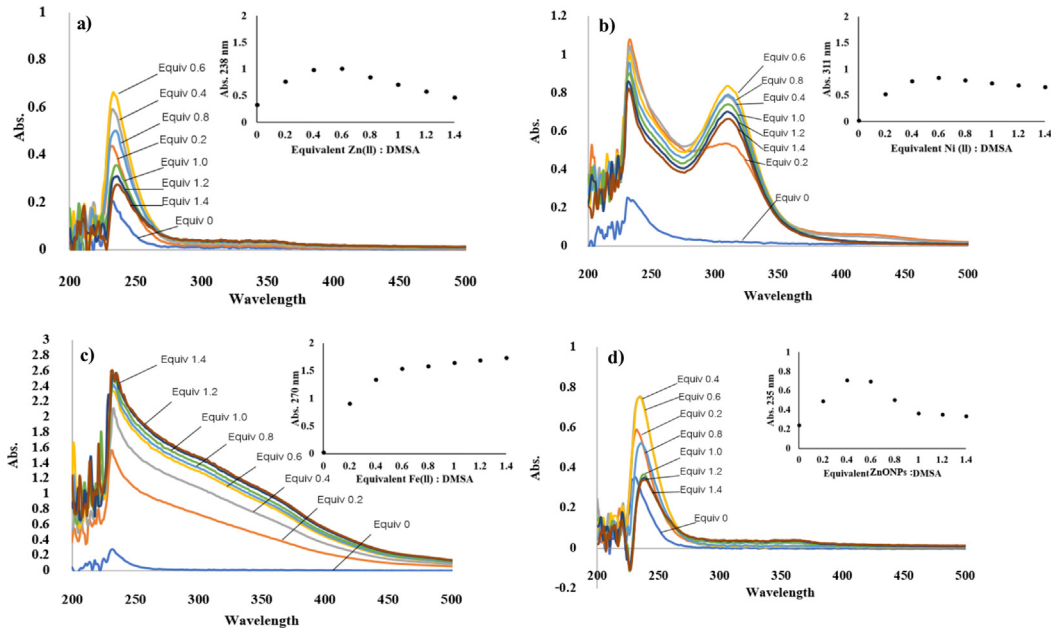

Figure 5. UV–Vis spectral titration of DMSA in DMSA after the addition of metal ions: (a) Zn(II), (b) Ni(II), (c) Fe(II) and (d) ZnONPS. Inset: the stoichiometry analysis between DMSA and metal ions by molar ratio.

mole-ratio plot show the maximum absorption of ZnONPs/DMSA = 0.5, which indicated the formation of ZnONPs with a complex DMSA ratio of 1:2 (Figure 5d).

From mentioned results, the UV titration results showed that DMSA reacted with metal ions to form Zn(II)-DMSA, Ni(II)-DMSA and ZnONPs-DMSA with a ratio of 1:2 complexes. According to Hard-Soft Acid Base Theory (HSAB), Ni(II), Fe(II) and Zn(II) were borderline and –SH are soft base, but –COOH are hard base. Fe(II) reacted with carboxyl (COO-) of two DMSA to form Fe(II)-DMSA with a ratio of 1:2 complexes. As shown in previous results, the studied on the complex formation of Ni(II), Zn(II) and Fe(II) with DMSA showed the formation of metal ion:DMSA with a ratio of 1:2 complex (Fang and Fernando, 1995; Lappin and McAuley, 1978; Egorova et al., 1972; Chen et al., 2015; Kim and Starthmann, 2007). According to the result of FTIR spectra was attributed to the possible conformational of metal ion-DMSA complex (Fang and Fernando, 1994; Soler et al., 2011). This metal-binding was found to form complexes which structures are depended on the metal ion to be complexed.

Additionally, the results of metal-DMSA complexes were investigated by using DFT calculation which the Ni(II)-DMSA complex (2a) is more stable than the Zn(II)-DMSA complex and Fe(II)-DMSA complex with the binding energy of -1553.46, -1500.78 and -1068.82 kcal mol^{-1}, respectively which indicates the coordination of carboxyl groups to the metal atom in the complexes. In order to confirm complex formation between DMSA and ZnONPs, IR vibrational frequency show the asymmetric and symmetric stretching modes of carboxylate at around 1568 and 1386 cm^{-1} indicating the interaction between DMSA and ZnONPs.

Furthermore, the determination of the stability constant of the DMSA complex with ZnONPs and other metal ions were calculated by the Benesi-Hildebrand equation presented in Table 2 indicated the stabilities of the metal chelates of DMSA were Zn(II) > ZnONPs > Ni(II) > Fe(II) (Aposhian, 1983; Ma et al., 2018).

3.5. Theoretical investigations

3.5.1. Geometries of DMSA structure

DMSA were optimized with DFT using the B3LYP functional within the 6-31G (d,p) basis set for 2 possible structures such as 2S, 3S and 2R, 3S conformation. The total energy values show that the most stable structure of *meso*-DMSA was 2R, 3S conformation, as shown in Figure 6.

3.5.2. Structure of Metal-DMSA complexes

The structural of complex formation between metal ions (Ni(II), Fe(II) and Zn(II)) and DMSA are presented in Figures 7, 8, and 9. In order to investigate complex formation between DMSA and metal ions, three coordination binding sites were considered (2OH, 2SH and 2OS form). In case of 2OH and 2SH forms, metal ions are coordinated by carboxyl group (–COOH) (Figure 7) and thiol group (-SH) (Figure 8) of DMSA, respectively. While the 2OS form, DMSA forms a complex with metal ions by carboxylic group (–COOH) and thiol group (–SH) (Figure 9). All of these three types were studied for 4 possible charges, such as +2, 0, -2 and -6 charge.

The metal-ligand binding energy (ΔE) of complexes, calculated by the difference between the energy of complex with the optimized geometry ($E_{complex}$) and the energies of the optimized ligands (E_L) and the metal

Table 2. Stability constant obtained from the Benesi-Hildebrand equation by UV-vis titration.

Complex	Stability constant (K)	Ratio of metal to ligand
Zn(II)-DMSA	4.81	1: 2
Ni(II)-DMSA	4.15	1: 2
Fe(II)-DMSA	3.58	1: 2
ZnONPs-DMSA	4.21	1: 2

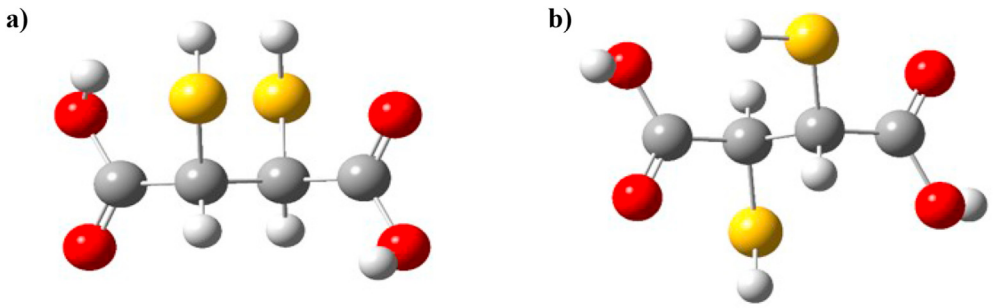

Figure 6. Structure of (a) DMSA (2S, 3S) and (b) DMSA (2R, 3S).

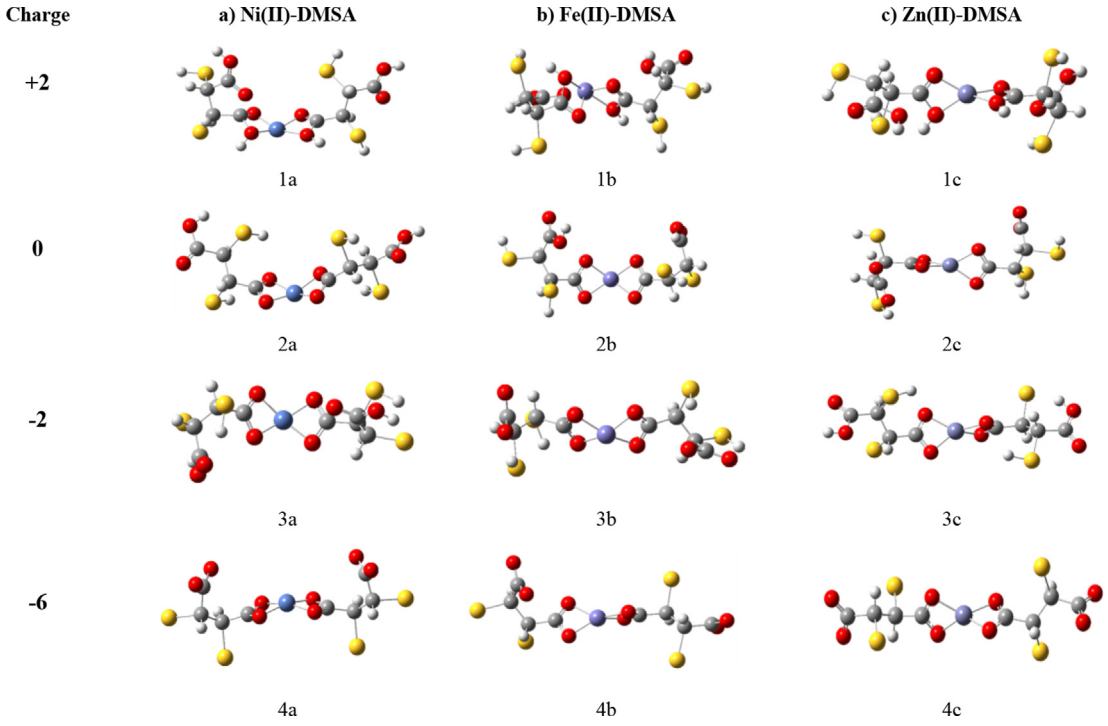

Figure 7. The interaction of Metal-DMSA complexes for 2OH form.

ions (E_M), were calculated according to Eq. (1) (Hernández-Valdés et al., 2017).

$$\Delta E = E_{complex} - (E_L + E_M) \quad (1)$$

DFT calculations were performed using the B3LYP functional were employed to investigate the ability of the DMSA chelating agent for the complex of Ni(II), Fe(II) and Zn(II) metal ions. The stable structure of *trans*-DMSA complex with metal ions were studied for 4 charge such as +2, 0, -2 and -6 in coordination binding sites of 2OH, 2SH and 2OS. Comparison in the stable structure of DMSA-Zn(II), DMSA-Ni(II) and DMSA-Fe(II) complex were classified by 4 charge such as +2, 0, -2 and -6 as shown in Table 3. We found that a charge of +2 show the stable structures in order of DMSA-Ni(II) > DMSA-Fe(II) > DMSA-Zn(II). The most stable structure was DMSA -Ni(II) which the Ni(II) reacts with DMSA by –SH and –COOH, with the binding energy of complex (9a) about -419.02 kcal mol^{-1}. For 0 charge, the stable structures were in order DMSA-Ni(II) > DMSA-Zn(II) > DMSA-Fe(II). Whereas, the DMSA-Ni(II) complex was the most stable with the binding energy of complex (2a) about -1553.46 kcal mol^{-1} that the Ni(II) reacts with DMSA by –COOH. For -2 and -6 charge, the stable structures were in order DMSA-Ni(II) > DMSA-Zn(II) > DMSA-Fe(II). A charge of -2, the DMSA-Ni(II) complex showed Ni(II)reacts with DMSA by –COOH, according to the binding energy of complex (3a) about -876.53 kcal mol^{-1}. Meanwhile, the charge of -6 the Ni(II) also reacts with DMSA by –COOH with the binding energy of the complex (4a) about -947.67 kcal mol^{-1}.

In addition, the stability of the complexes in 2OH form are more stable than that of 2SH and 2SH form, revealing in the complex formation of DMSA with Ni(II), Zn(II) and Fe(II) through 2OH form with a charge of 0. According to the study on the interaction between metal ions and DMSA complexes, it appeared that complex (2a) was more stable than complex (2c) and complex (2b) with a binding energy of -1553.46, -1500.78 and -1068.82 kcal mol^{-1},respectively as shown in Figure 7 and Table 3. The outcomes of theoretical calculations and the UV titration and infrared spectra experimental of metal ion-DMSA that verify the complex formations between metal ions and DMSA. The metal ion interact via the hydrogen bonding of the carboxylic groups of DMSA. Therefore, the results of this work demonstrate good candidate for treatment of Ni(II), Zn(II), Fe(II)and ZnONPs poisoning.

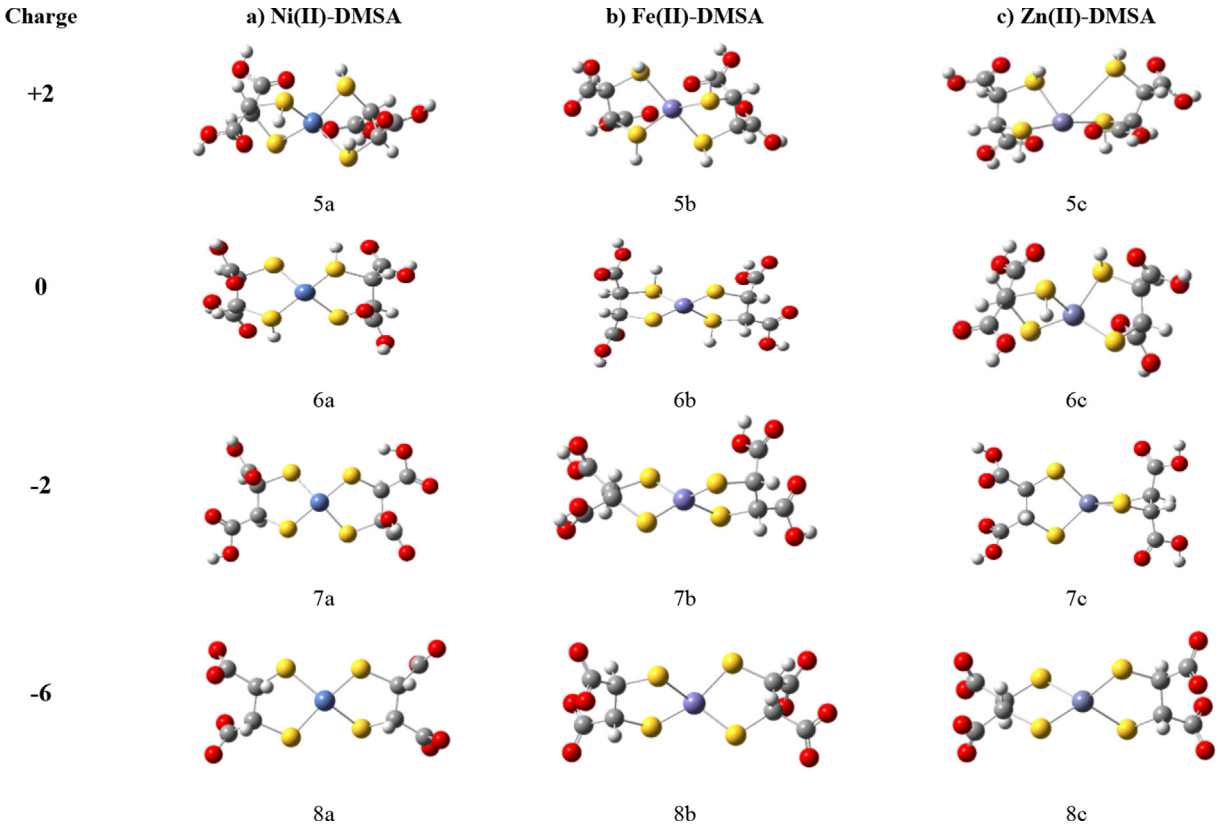

Figure 8. The interaction of Metal-DMSA complexes for 2SH form.

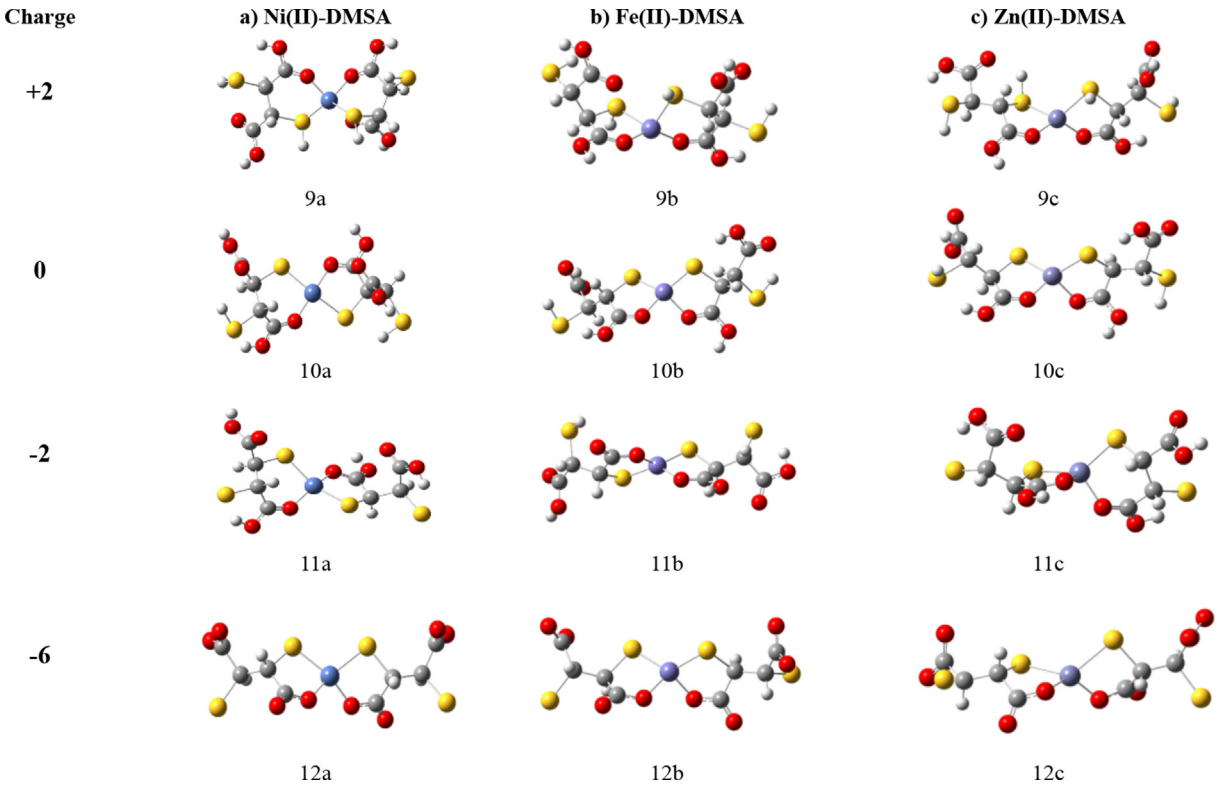

Figure 9. The interaction of Metal-DMSA complexes for 2OS form.

Table 3. Calculated values (in kcal mol^{-1}) of the metal ions-DMSA complex.

Complex	Charge	Binding energy (Kcal mol^{-1})
1a	+2	−370.47
1b	+2	−327.47
1c	+2	−315.05
5a	+2	−397.51
5b	+2	−376.77
5c	+2	−379.56
9a	+2	−419.02
9b	+2	−345.23
9c	+2	−351.04
2a	0	−1553.46
2b	0	−1068.82
2c	0	−1500.78
6a	0	−666.43
6b	0	−623.40
6c	0	−627.31
10a	0	−675.51
10b	0	−627.81
10c	0	−629.82
3a	−2	−876.53
3b	−2	−787.19
3c	−2	−821.85
7a	−2	−805.93
7b	−2	−761.81
7c	−2	−759.00
11a	−2	−828.48
11b	−2	−773.81
11c	−2	−783.99
4a	−6	−947.67
4b	−6	−880.53
4c	−6	−914.89
8a	−6	−873.58
8b	−6	−849.90
8c	−6	−871.03
12a	−6	−929.83
12b	−6	−875.52
12c	−6	−895.41

4. Conclusion

The interaction of DMSA with metal ions and ZnONPs were studied. The ZnONPs and DMSA-ZnONPs were synthesized by a cost effective and simple co-precipitation method from $ZnCl_2$ and confirmed by UV-Vis spectroscopy, FTIR spectroscopy and SEM. In the UV-Vis spectroscopic study, ZnONPs and DMSA-ZnONPs showed absorbance at 361 and 322 nm, respectively. For the FTIR spectroscopic study, the ZnONPs showed that the characteristic absorption peaks at 475 cm^{-1} and the DMSA-ZnONPs showed absorption peaks at 474 cm^{-1} of Zn–O, at 3388 cm^{-1} of –OH and 1574 and 1386 cm^{-1} of carboxylate. Moreover, the SEM indicated the size of ZnONPs and DMSA-ZnONPs were 40 and 25 nm, respectively. Through the UV titration experiment, by Job's method, we found that the formation of the DMSA complexes with ZnONPs being the ratio of 1:2. For the determination of stability constant of the DMSA complex, ZnONPs were calculated by the Benesi-Hildebrand equation and showed 4.21. This value indicated the high ability of DMSA as a chelating agent due to DMSA, which were able to form complexes with metal in nanosized with a high stability constant. In the case of UV titration metal ions-DMSA complex, we found that Zn(II), Ni(II) and Fe(II) also formed a complex with a DMSA ratio of 1:2. Due to dithiol (-SH) of DMSA were reacted with Zn(II) and Ni(II) while the carboxyl (-COOH) of DMSA were reacted with Fe(II). Moreover, a comparison between the stable structure of DMSA-Zn(II), DMSA-Ni(II) and DMSA-Fe(II) complex classified by 4 charges, such as +2, 0, -2 and -6. We found that the most stable structure in the interaction between metal ions and DMSA complexes and it appeared that complex 2a was more stable than other complexes with a binding energy of -1553.46 kcal mol^{-1}. Therefore, UV titration and the computational chemistry results led to a prediction about the possible structure of the DMSA complex with metal ions. The results indicated efficiency and the stability of DMSA with metal ions and ZnONPs in therapeutic chelating agents. Thus, DMSA is an interesting option for the treatment of heavy metal and nanoparticles poisoning in patients due to high efficiency and high stability.

Declarations

Author contribution statement

Sujittra Srisung: Conceived and designed the experiments; Analyzed and interpreted the data; Contributed reagents, materials, analysis tools or data; Wrote the paper.

Poonyawee Keattanong: Performed the experiments; Wrote the paper.

Nootcharin Wasukan: Performed the experiments; Analyzed and interpreted the data; Wrote the paper.

Mayuso Kuno: Analyzed and interpreted the data; Contributed reagents, materials, analysis tools or data.

Funding statement

The authors gratefully acknowledge Srinakharinwirot University. We extend our gratitude to National Science and Technology Development Agency (NSTDA) for their valuable supports.

Data availability statement

The authors do not have permission to share data.

Declaration of interests statement

The authors declare no conflict of interest.

Additional information

No additional information is available for this paper.

Acknowledgements

This work was supported by the Department of Chemistry, Faculty of Science, Srinakharinwirot University.

References

Alamdari, S., Ghamsari, M.S., Lee, C., Han, W., Park, H.-H., Tafreshi, M.J., Afarideh, H., Ara, M.H.M., 2020. Preparation and Characterization of zinc oxide nanoparticles using leaf extract of *Sambucus ebulus*. Appl. Sci. 10, 3620.

Ali, H., Khan, E., Ilahi, I., 2019. Environmental chemistry and ecotoxicology of hazardous heavy metals: environmental persistence, toxicity, and bioaccumulation. J. Chem. 14.

Aposhian, V., 1983. DMSA and DMPS-water soluble antidotes for heavy metal poisoning. Annu. Rev. Pharmacol. Toxicol. 23, 193–213.

Aposhian, H.V., Maiorino, R.M., Gonzalez-Ramirez, D., Zuniga-Charles, M., Xu, Z., Hurlbut, K.M., Junco-Munoz, P., Dart, R.C., Aposhian, M.M., 1995. Mobilization of heavy metals by newer, therapeutically useful chelating agents. Toxicol 97, 23–38.

Arunakumara, K.K.I.U., Walpola, B.C., Yoon, M.-H., 2013. Current status of heavy metal contamination in Asia's rice lands. Rev. Environ. Sci. Biotechnol. 12 (4), 355–377.

Biltek, S.R., Mandal, S., Sen, A., Reber, A.C., Pedicini, A.F., Khanna, S.N., 2003. Synthesis and structural characterization of an atom-precise bimetallic nanocluster, $Ag_4Ni_2(DMSA)_4$. J. Am. Chem. Soc. 135 (1), 26–29.

Heavy Metals in the Environment: Origin, Interaction and Remediation. In: Bradl, H. (Ed.), 2002, 6. Academic Press, London.

Campbell, J.R., Clarkson, T.W., Omar, M.D., 1986. The therapeutic use of 2,3-dimercaptopropane-1-sulfonate in two cases of inorganic mercury poisoning. J. Am. Med. Assoc. 256, 3127–3130.

Cavanillas, S., Chekmeneva, E., Ariño, C., Díaz-Cruz, J.M., Esteban, M., 2012. Electroanalytical and isothermal calorimetric study of as (III) complexation by the metal poisoning remediators, 2, 3- dimercapto-1-propanesulfonate and meso-2, 3-dimercaptosuccinic acid. Anal. Chim. Acta 746, 47–52.

Chen, W., Cao, F., Zheng, W., Tian, Y., Xianyu, Y., Xu, P., Zhang, W., Wang, Z., Deng, K., Jiang, X., 2015. Detection of the nanomolar level of total Cr[(III) and (VI)] by functionalized gold nanoparticles and a smartphone with the assistance of theoretical calculation models. Nanoscale 7, 2042–2049.

Egorova, L.G., Okonishnikova, I.E., Nirenburg, V.L., Postovskii, I. Ya., 1972. Complex formation of certain metals with dimercaptosuccinic acid stereoisomers. J. Pharmaceut. Chem. J. 6, 79–81.

Fang, X., Fernando, Q., 1994. A Comparative study of *meso*- and rac-2,3-Dimercaptosuccinic acids and their zinc complexes in aqueous solution. Chem. Res. Toxicol. 7, 770–778.

Fang, X., Fernando, Q., 1995. Stereoisomeric selectivity of 2,3-dimercaptosuccinic acids in chelation therapy for lead poisoning. Chem. Res. Toxicol. 7, 525–536.

Fang, X., Hua, F., Fernando, Q., 1996. Comparison of *rac*- and *meso*-2,3-Dimercaptosuccinic acids for chelation of mercury and cadmium using chemical speciation models. Chem. Res. Toxicol. 9, 284–290.

Fortunato, E., Gonçalves, A., Pimentel, A., Barquinha, P., Gonçalves, G., Pereira, L., Ferreira, I., Martins, R., 2009. Zinc oxide a multifunctional material: from material to device applications. Appl. Phys. 96, 197–205.

Frisch, M.J., Trucks, G.W., Schlegel, H.B., Scuseria, G.E., Robb, M.A., Cheeseman, J.R., Montgomery Jr., J.A., Vreven, T., Kudin, K.N., Burant, J.C., Millam, J.M., Iyengar, S.S., Tomasi, J., Barone, V.B., Mennucci, M., Cossi, G., Scalmani, N., Rega, G.A., Petersson, Nakatsuji, H., Hada, M., Ehara, M., Toyota, K., Fukuda, R., Hasegawa, J., Ishida, M., Nakajima, T., Honda, Y., Kitao, O., Nakai, H., Klene, M., Li, X., Knox, J.E., Hratchian, H.P., Cross, J.B., Adamo, C., Jaramillo, J., Gomperts, R., Stratmann, R.E., Yazyev, O., Austin, A.J., Cammi, R., Pomelli, C., Ochterski, J.W., Ayala, P.Y., Morokuma, K., Voth, G.A., Salvador, P., Dannenberg, J.J., Zakrzewski, V.G., Dapprich, S., Daniels, A.D., Strain, M.C., Farkas, O., Malick, D.K., Rabuck, A.D., Raghavachari, K., Foresman, J.B., Ortiz, J.V., Cui, Q., Baboul, A.G., Clifford, S., Cioslowski, J., Stefanov, B.B., Liu, G., Liashenko, A., Piskorz, P., Komaromi, I., Martin, R.L., Fox, D.J., Keith, T., Al-Laham, M.A., Peng, C.Y., Nanayakkara, A., Challacombe, M., Gill, P.M.W., Johnson, B., Chen, W., Wong, M.W., Gonzalez, C., Pople, J.A., 2003. Gaussian 03, Revision B.01. Gaussian Inc, Pittsburgh PA.

Harris, W.R., Chen, Y., Stenback, J., Shah, B., 1991. Stability constants for dimercaptosuccinic acid with bismuth (III), zinc (II), and lead (II). J. Coord. Chem. 23, 173–186.

Hernández-Valdés, D., Blanco-González, A., García-Fleitas, A., Rodríguez-Riera, Meola, Z.G., Alberto, R., Jáuregui-Haza, U., 2017. Insight into the structure and stability of Tc and Re DMSA complexes: a computational Study. J. Mol. Graph. Model. 71, 167–175.

He, Z.L., Yang, X.E., Stoffella, P.J., 2005. Trace elements in agroecosystems and impacts on the environment. J. Trace Elem. Med. Biol. 19 (2–3), 125–140.

Jahromi, E.Z., Gailer, J., Pickering, I.J., George, G.N., 2014. Structural characterization of Cd^{2+} complexes in solution with DMSA and DMPS. J. Inorg. Biochem. 136, 99–106.

Jeevanandam, J., Barhoum, A., Chan, Y.S., Dufresne, A., Danquah, M.K., 2018. Review on nanoparticles and nanostructured materials: history, sources, toxicity and regulations. Beilstein J. Nanotechnol. 9, 1050–1074.

Khan, I., Saeed, K., Khan, I., 2019. Nanoparticles: properties, applications and toxicities. Arab. J. Chem. 12, 908–993.

Kim, D., Starthmann, T.J., 2007. Role of organically complexed iron(II) species in the reductive transformation of RDX in anoxic environments. Environ. Sci. Technol. 41, 1257–1264.

Kołodziejczak-Radzimska, A., Jesionowski, T., 2014. Zinc oxide—from synthesis to application. Rev. Mater. 7, 2833–2881.

Lanje, A.S., Sharma, S.J., Ningthoujam, R.S., Ahn, J.-S., Pode, R.B., 2013. Low temperature dielectric studies of zinc oxide (ZnO) nanoparticles prepared by precipitation method. Adv. Powder Technol. 24, 331–335.

Lappin, A.G., McAuley, A., 1978. Reactions between Copper(ii) and 2-Mercaptosuccinic acid in aqueous perchlorate solution. J.C.S. Dalton. 7, 1606–1609.

Lee, K.J., Nallathamby, P.D., Browning, L.M., Osgood, C.J., Xu, X.-H.N., 2007. In vivo imaging of transport and biocompatibility of single silver nanoparticles in early development of zebrafish embryos. ACS Nano 1, 133–143.

Lorenz, C., Windler, L., Goetz, N.V., Lehmann, R.P., Schuppler, M., Hungerbuehler, K., Heuberger, M., Nowack, B., 2012. Characterization of silver release from commercially available functional (nano)textile. Chemosphere 89, 817–824.

Ma, R., Li, Q., Zhang, Q. Indian., 2018. A novel selective chemosensor for Mg^{2+} detection based on quinoline- hydrazone-crown ether. J. Chem. Soc. B 120–126.

Nahhal, El I., Elmanama, M., A, A., Amara, N.M., 2016. Synthesis of nanometal oxide-coated cotton composites. Cotton Res. 279–297.

Pillai, A.M., Sivasankarapillai, V.S., Rahdar, A., Joseph, J., Sadeghfar, F., Anuf, R.A., Rajesh, K., Kyzas, G.Z., 2020. Green synthesis and characterization of zinc oxide nanoparticles with antibacterial and antifungal activity. J. Mol. Struct. 1211, 128107.

Rad, S.S., Sani, A.M., Mohseni, S., 2019. Biosynthesis, characterization and antimicrobial activities of zinc oxide nanoparticles from leaf extract of *Mentha pulegium (L.)*. Microb. Pathog. 131, 239–245.

Ramos, A.P., Cruz, M.A.E., Tovani, C.B., Ciancaglini, P., 2017. Biomedical applications of nanotechnology biophys rev, 9, pp. 79–89.

Rao, N.S., Rao, M.V.B., 2015. Structural and Optical Investigation of ZnO nanopowders synthesized from zinc chloride and zinc nitrate. Am. J. Mater. Sci. 5, 66–68.

Rivera, M., Zheng, W., Aposhian, H.V., Frenando, Q., 1989. Determination and metabolism of dithiol chelating agents VIII. Metal complexes of meso-Dimercaptosuccinic Acid. Toxicol. Appl. Pharmacol. 100, 96–106.

Sevinc, E., Ertas, F.S., Ulusoy, G., Ozen, C., Acar, H.Y., 2012. *Meso*-2,3-dimercaptosuccinic acid: from heavy metal chelation to CdS quantum dots. J. Mater. Chem. 22, 5137–5144.

Sfakianakis, D.G., Renieri, E., Kentouri, M., Tsatsakis, A.M., 2015. Effect of heavy metals on fish larvae deformities: a review. Environ. Res. 137, 246–255.

Soler, M.A.G., Lima, E.C.D., Nunes, E.S., Silva, F.L.R., Oliveira, A.C., Azevedo, R.B., Morais, P.C., 2011. Spectroscopic study of maghemite nanoparticles surface-grafted with DMSA. J. Phys. Chem. 115, 1003–1008.

Spuches, A.M., Kruszyna, H.G., Rich, A.M., Wilcox, D.E., 2005. Thermodynamics of the As(III)-Thiol Interaction: arsenite and monomethylarsenite complexes with glutathione, dihydrolipoic acid, and other thiol ligands. Inorg. Chem. 44, 2964–2972.

Trivedi, M.K., Sethi, K.K., Panda, P., Jana, S., 2017. A comprehensive physicochemical, thermal, and spectroscopic characterization of zinc (II) chloride using X-ray diffraction, particle size distribution, differential scanning calorimetry, thermogravimetric analysis/differential thermogravimetric analysis, ultraviolet-visible, and Fourier transform-infrared spectroscopy. Int. J. Pharma. Investig. 7, 33–40.

Vance, M.E., Kuiken, T., Vejerano, E.P., McGinnis, S.P., Hochella Jr., M.F., Rejeski, D., Hull, M.S., 2015. Nanotechnology in the real world: redeveloping the nanomaterial consumer products inventory. Beilstein J. Nanotechnol. 6, 1769–1780.

Wasukan, N., Srisung, S., Kuno, M., Kulthong, K., Maniratanachote, R., 2015. Interaction evaluation of silver and dithizone complexed using DFT calculations and NMR analysis. Spectrochim. Acta. Mol. Biomol. Spectros. 149, 830–838.

Willander, M., 2014. Zinc Oxide Nanostructures: Advances and Applications, first ed. Pan Stanford, New York, NY, USA.